Environment International 126 (2019) 171–183

Contents lists available at ScienceDirect

Environment International

journal homepage: www.elsevier.com/locate/envint

The carbonaceous aerosol levels still remain a challenge in the Beijing-Tianjin-Hebei region of China: Insights from continuous high temporal resolution measurements in multiple cities

Dongsheng Ji[a,b,*], Meng Gao[c], Willy Maenhaut[d,*], Jun He[e], Cheng Wu[f,g], Linjun Cheng[h], Wenkang Gao[a], Yang Sun[a,b], Jiaren Sun[i], Jinyuan Xin[a,b], Lili Wang[a,b], Yuesi Wang[a,b]

[a] State Key Laboratory of Atmospheric Boundary Layer Physics and Atmospheric Chemistry, Institute of Atmospheric Physics, Chinese Academy of Sciences, Beijing 100191, China
[b] Atmosphere Sub-Center of Chinese Ecosystem Research Network, Institute of Atmospheric Physics, Chinese Academy of Sciences, Beijing 100191, China
[c] John A. Paulson School of Engineering and Applied Sciences, Harvard University, Cambridge, MA 02138, USA
[d] Department of Chemistry, Ghent University, Gent 9000, Belgium
[e] International Doctoral Innovation Centre, Department of Chemical and Environmental Engineering, University of Nottingham Ningbo China, Ningbo 315100, China
[f] Institute of Mass Spectrometer and Atmospheric Environment, Jinan University, Guangzhou 510632, China
[g] Guangdong Provincial Engineering Research Center for On-Line Source Apportionment System of Air Pollution, Guangzhou 510632, China
[h] China National Environmental Monitoring Center, Beijing 100012, China
[i] South China Institute of Environmental Sciences, Ministry of Environmental Protection, Guangzhou 510655, China

ARTICLE INFO

Handling Editor: Xavier Querol

ABSTRACT

Carbonaceous aerosols in high emission areas attract worldwide attention of the scientific community and the public due to their adverse impacts on the environment, human health and climate. However, long-term continuous hourly measurements are scarce on the regional scale. In this study, a one-year hourly measurement (from December 1, 2016 to November 30, 2017) of organic carbon (OC) and elemental carbon (EC) in airborne fine particles was performed using semi-continuous OC/EC analyzers in Beijing, Tianjin, Shijiazhuang and Tangshan in the Beijing-Tianjin-Hebei (BTH) region in China, which is one of high emission areas in China, even in the world. Marked spatiotemporal variations were observed. The highest concentrations of OC (22.8 ± 30.6 μg/m^3) and EC (5.4 ± 6.5 μg/m^3) occurred in Shijiangzhuang while the lowest concentrations of OC (11.0 ± 10.7 μg/m^3) and EC (3.1 ± 3.6 μg/m^3) were obtained in Beijing and Tianjin, respectively. Pronounced monthly, seasonal and diurnal variations of OC and EC were recorded. Compared to published data from the past two decades for the BTH region, our OC and EC levels were lower, implying some effect of recent measures for improving the air quality. Significant correlations of OC versus EC ($p < 0.001$) were found throughout the study period with high slopes and correlation coefficients in winter, but low slopes and correlation coefficients in summer. The estimated secondary OC (SOC), based on the minimum R squared (MRS) method, represented 29%, 47%, 38% and 48% of the OC for Beijing, Tianjin, Shijiazhuang and Tangshan, respectively. These percentages are larger than previous ones obtained for the BTH region in the past decade. There were obvious differences in the potential source regions of OC and EC among the four cities. Obvious prominent potential source areas of OC and EC were observed for Beijing, which were mainly located in the central and western areas of Inner Mongolia and even extended to the Mongolian regions, which is different from the findings in previous studies. For all sites, adjacent areas of the main provinces in northern China were found to be important potential source areas.

1. Introduction

Carbonaceous aerosols, which consist of organic carbon (OC) and elemental carbon (EC), play an important role in climate change, environmental degradation and public health risks. They affect the Earth's radiation balance directly (most of the OC scatters solar and terrestrial radiation while EC and brown carbon absorb solar radiation) (Bond et al., 2013) and indirectly (OC and EC can modify the

* Corresponding authors: D. Ji, State Key Laboratory of Atmospheric Boundary Layer Physics and Atmospheric Chemistry, Institute of Atmospheric Physics, Chinese Academy of Sciences, Beijing 100191, China; W. Maenhaut, Department of Chemistry, Ghent University, Gent 9000, Belgium.
E-mail addresses: jds@mail.iap.ac.cn (D. Ji), Willy.Maenhaut@UGent.be (W. Maenhaut).

https://doi.org/10.1016/j.envint.2019.02.034
Received 10 January 2019; Received in revised form 11 February 2019; Accepted 12 February 2019
Available online 22 February 2019

microphysical properties of clouds through their role as cloud condensation nuclei and/or ice nuclei) (IPCC, 2013; Bond and Bergstrom, 2006; Menon et al., 2005). OC and EC also lead to reduced visibility (Ji et al., 2017; Li et al., 2019) and they account for a high proportion of fine particulate matter (aerosols with aerodynamic diameter < 2.5 μm, $PM_{2.5}$) (Seinfeld and Pandis, 2016). Particulate organic compounds have been identified as a possible health hazard; for example, polyaromatic hydrocarbons (PAHs) have shown to be carcinogenic for humans and animals (IARC, 2010; Grimmer, 2018). EC, as a universal carrier of PAHs and heavy metals, has adverse effects on the human body such as the lungs, the body's major defense cells, and possibly the systemic blood circulation (Mills et al., 2005). Risk of cardiovascular admissions is also associated with EC (Peng et al., 2009). Therefore, OC and EC have drawn worldwide attention in recent years due to their impacts on the environment, human health, and climate (Bond et al., 2013; Ding et al., 2016; Hansen et al., 2005).

The Beijing-Tianjin-Hebei (BTH) region in China is a major source region of carbonaceous aerosols because of the high consumption of fossil fuels and bio-fuels (Cao et al., 2006; Junker and Liousse, 2008). Much attention has been devoted to establishing emission inventories for OC and EC in China (Fig. S1, Supplementary material). Zhao et al. (2013) studied the characteristics of OC and EC in the BTH region and found that the average annual OC and EC concentrations in Shangdianzi (background), Beijing, Tianjin, Chengde, and Shijiazhuang (urban) were in the range of 10.8–26.4 μg/m^3 and 3.9–9.7 μg/m^3, respectively, and that the carbonaceous aerosol pollution was spatially similar and seasonally-dependent. Wang et al. (2015a) investigated the seasonal variation and source apportionment of $PM_{2.5}$ carbonaceous aerosol in the Beijing and Tangshan cities of China, and they showed that the carbonaceous materials accounted for 17.3–21.2% of the $PM_{2.5}$ and that coal combustion, vehicle exhaust and biomass burning were the main sources. Huang et al. (2017) found that organic matter (OM = OC × 1.6) and EC represented 16.0–25.0% and 2.8–6.3% of the $PM_{2.5}$ at three urban sites (Beijing, Tianjin, and Shijiazhuang) and a regional background site (Xinglong), and that OM and EC exhibited the largest concentrations and contributions in winter. However, the above studies were carried out based on filter sampling with a low time resolution, which do not fully shed light on the detailed characteristics of OC and EC. To grasp more complete information on the variation, evolution and sources of the carbonaceous aerosol in the BTH region, high time-resolved, continuous and in situ measurements need to be carried out at multiple sites. However, systematic studies supported by high time resolution observation about the occurrence levels, spatial and seasonal variation, distribution and sources of carbonaceous aerosols in $PM_{2.5}$ in the BTH region are still scarce.

In this study, OC and EC in $PM_{2.5}$ were measured in Beijing, Tianjin, Shijiazhuang and Tangshan, which represent typical urban cities in the BTH region of China. The characteristics of the OC and EC pollution and their seasonal and diurnal variations are discussed. The relationship between OC and EC was examined and secondary organic carbon was estimated by the EC tracer method (Turpin and Huntzicker, 1995). In addition, the source areas of the carbonaceous aerosols were identified using the potential source contribution function (PSCF) method. This study presents a multiple site hourly time-resolved observation of OC and EC and provides invaluable information for evaluating the effects of air pollution on human health and climate as well as for optimizing the emission control strategies for the BTH region in China.

2. Experimental

2.1. Sampling sites

As depicted in Fig. 1, four cities in the BTH region were selected for the current study. Beijing and Tianjin are direct-controlled municipalities surrounded by the Hebei province. Shijiazhuang is the capital of the Hebei province and Tangshan is an important industrial city in northern China. The sampling campaign was conducted from December 1, 2016 to November 30, 2017. The urban sampling site in Beijing (39°58′28″N, 116°22′16″E, 44 m a.s.l.) is located inside the campus of the State Key Laboratory of Atmospheric Boundary Layer Physics and Atmospheric Chemistry (LAP/CERN), Institute of Atmospheric Physics (IAP), Chinese Academy of Sciences (CAS). The urban sampling site in Tianjin (39°4′30″ N, 117°12′22″ E, −9 m a.s.l.) is located in the park of the Tianjin Institute of Meteorological Science in the Hexi district of Tianjin. The urban sampling site in Shijiazhuang (38°1′40″N, 114°31′45″E, 70 m a.s.l.) is located on the roof of the main building at the Hebei Provincial Meteorological Bureau. The urban sampling site in Tangshan (39°37′25″N, 118°9′20″E, 14 m a.s.l.) is located on the top of the building at the College of Materials Science and Engineering in Hebei Polytechnic University. A detailed description on the above four cities is given in the Supplementary material.

2.2. Instrumentation

The OC and EC levels in $PM_{2.5}$ were measured hourly with a semi-continuous thermal-optical transmittance (TOT) based OC/EC analyzer (RT-4, Sunset Laboratory Inc., Tigard, Oregon, USA). An inline parallel carbon denuder that removes volatile organic gases was installed upstream of the analyzer. Aerosol particles were collected on a round 16-mm diameter quartz fibre filter (Tissuquartz 2500 QAT-UP, Pall Corporation, MI, USA), which is located in the oven, at a sampling flow rate of 8 L/min. After 30 min collection, the oven of the instrument was purged with helium and the temperature was increased in multiple programmed steps based on a modified NIOSH thermal protocol (Birch and Cary, 1996). Particulate organic carbon was then thermally volatilized and oxidized to carbon dioxide (CO_2), which was quantified using a non-dispersive infrared (NDIR) detector. The oven was cooled prior to the second part of the analysis, when the oven was purged with a mixture of 5% oxygen in helium; and then the sample was again heated incrementally. During this stage, all of the remaining carbon on the filter, including elemental carbon, was oxidized to CO_2, which was also measured using the NDIR. For charring correction, a He−Ne laser beam monitored the sample transmittance throughout the heating process. When the intensity of the laser signal returned to its initial value, the split point between OC and EC was set (Birch and Cary, 1996). The maintance and calibration were strictly performed according to the Standard Operating Procedure (https://ebas-submit.nilu.no/Standard-Operating-Procedures). The uncertainty of the total carbon (TC = OC + EC) measurement was estimated to be about 7%, determined by the standard error of the sucrose calibration and the internal standard methane calibration (Han et al., 2009). Uncertainties in the EC/OC split, which may depend on the temperature protocol, can lead to additional errors (Boparai et al., 2008).

A synchronized hybrid ambient real-time particulate monitor (Model SHARP 5030, Thermo-Fisher Scientific, Massachusetts, USA), a US EPA Federal Equivalent Method analyzer, was used throughout the entire one-year campaign to monitor $PM_{2.5}$. The accuracy for 24-h measurements was ± 5%. Calibration was performed and the glass fibre filter tape was replaced every 6 months.

2.3. Meteorological data and satellite data

Meteorological data, including hourly observational values of atmospheric temperature (*T*), pressure (*P*), relative humidity (RH), wind speed (*WS*) and precipitation, were downloaded from the China meteorological data service center (http://data.cma.cn/en). The monthly averaged data for Beijing, Tianjin, Shijiazhuang and Tangshan are given in Tables S1-S4. Of the four cities, Shijiazhuang had the highest *T* and the lowest *WS* with monthly average values varying from −0.7 to 28.5 °C and from 1.2 to 2.6 m/s, respectively. Tianjin had the highest *WS*, with monthly average values varying from 2.0 to 3.6 m/s. Tangshan had the highest RH with monthly average values varying from 43.9 to 79.7%, while the lowest RH values were observed in Beijing with monthly average values varying from 36.3 to 70.2%. Fire

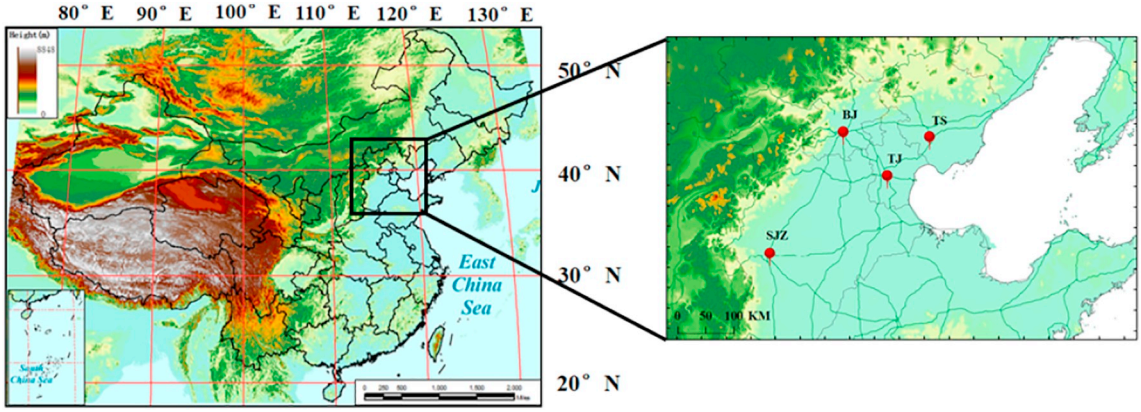

Fig. 1. Location of the sampling sites: Beijing (BJ), Tianjin (TJ), Shijiazhuang (SJZ), and Tangshan (TS).

spots data were derived from the MODIS Terra (collection 4) daily, thermal anomalies (MOD14A1) data set, which captured fire pixels from 10:30 to 13:30 (Giglio, 2005). In the present study, fire spots data used are for northern China.

2.4. Source area identification

The residence time probability analysis of Ashbaugh et al. (1985), also known as the 'PSCF' method, has been extensively used in the identification of source locations and preferred transport pathways of atmospheric trace elements and particulate species (e.g., Poirot and Wishinski, 1986; Polissar et al., 2001; Lupu and Maenhaut, 2002). PSCF uses backward trajectories to determine potential locations of emission sources. In a nutshell, PSCF is defined as the probability that an air parcel with concentration higher than a specified threshold arrives at the receptor site after having resided in a certain grid cell of the spatial domain of interest (Lupu and Maenhaut, 2002). The PSCF is defined as:

$$\mathrm{PSCF}(i,j) = w_{ij} \times (m_{ij}/n_{ij}) \quad (1)$$

where n_{ij} is the total number of back-trajectory segment endpoints that fall into the grid cell (i, j) over the period of study, m_{ij} is the number of endpoints in (i, j) with concentration values at the receptor site exceeding a specified threshold value, and w_{ij} is an empirical weight function proposed to reduce the uncertainty of n_{ij} during the study period. Higher ratios of m_{ij}/n_{ij} illustrate higher probability of particular grids through which passing air masses will lead to a concentration at the receptor site.

The National Oceanic and Atmospheric Administration Hybrid Single-Particle Lagrangian Integrated Trajectory model (HYSPLIT 4.9) (Draxler and Rolph, 2003) was used for calculating the 48-h backward trajectories terminating at the study site at a height of 100 m every 1 h during the sampling period from 1 December 2016 to 30 November 2017. In this study, the domain for the PSCF was set in the range of (30–60°N, 65–150°E) with the grid cell size of 0.25 × 0.25°. The 75th percentiles for OC and EC for the whole study period and each season were used as threshold values to calculate m_{ij} (Sun et al., 2015). A weighting function (w_{ij}) introduced by Polissar et al. (1999) and Wang et al. (2009) was used to reduce the uncertainties for those grid cells with a limited number of endpoints over the entire one-year period.

3. Results and discussion

3.1. Annual average concentrations

The average concentrations and associated standard deviations for OC and EC over the study period were 11.0 ± 10.7 and 3.4 ± 3.3, 12.0 ± 9.8 and 3.1 ± 3.6, 22.8 ± 30.6 and 5.4 ± 6.5, and 12.1 ± 9.6 and 3.5 ± 3.6 μg/m^3 for Beijing, Tianjin, Shijiazhuang and Tangshan, respectively. The highest concentrations were observed in Shijiazhuang, which was associated with the energy structure that is highly dependent on coal consumption and also unfavorable meteorological conditions. When excluding Shijiazhuang, the OC data rank in the order Tangshan > Tianjin > Beijing while for EC the order is Tangshan > Beijing > Tianjin.

The contributions (mean ± standard deciation) of OC and EC to the measured $PM_{2.5}$ mass concentrations were, on average, 18.5 ± 12.7% and 5.8 ± 4.3%, 17.5 ± 13.5% and 4.6 ± 3.6%, 22.8 ± 11.2% and 5.3 ± 3.1%, and 16.7 ± 11.1% and 4.8 ± 3.7% for Beijing, Tianjin, Shijiazhuang and Tangshan, respectively. OC accounted for 75 ± 7%, 81 ± 7%, 80 ± 6% and 78 ± 6% of the TC for Beijing, Tianjin, Shijiazhuang and Tangshan, respectively, indicating that OC represents by far the major fraction of the carbonaceous aerosol. The average OC/EC ratios and associated standard deviations for the four sites were 3.5 ± 2.2, 4.3 ± 2.4, 4.7 ± 2.4 and 4.0 ± 1.7, respectively. The contributions of TC to the $PM_{2.5}$ mass were 24.3%, 22.0%, 28.1% and 21.5% for Beijing, Tianjin, Shijiazhuang and Tangshan, respectively; these percentages are similar to or slightly higher than earlier reported percentages for these four sites (Ji et al., 2016a, 2018; Jiang et al., 2017; Chen et al., 2017; Li and Bai, 2009; Gu et al., 2010; Wang et al., 2015a, 2015b; Wen et al., 2016). The slight increase in the TC/$PM_{2.5}$ mass ratios might suggest that the fraction of secondary inorganic ions like sulfate and nitrate from the conversion of NO_x and SO_2 in $PM_{2.5}$ has decreased relatively (Ji et al., 2016a, 2017, 2018). The results are also consistent with the decline in SO_2 and NO_x concentrations caused by the clean air act (http://english.sepa.gov.cn/Resources/Reports/). The carbonaceous aerosol levels were estimated as the sum of OC multiplied by 1.6 (Huang et al., 2017) and the EC concentration, and they accounted for 36%, 33%, 41% and 31% of the $PM_{2.5}$ values in Beijing, Tianjin, Shijiazhuang and Tangshan, respectively, indicating that the carbonaceous fractions provided a substantial contribution to the fine particle mass.

The variations of the OC and EC concentrations and of the OC/EC ratios as a function of the $PM_{2.5}$ concentration were examined. As shown in Fig. 2, six different air quality levels were defined, based on the $PM_{2.5}$ concentration, i.e., excellent ($0 < PM_{2.5} \leq 35$ μg/m^3), good ($35 < PM_{2.5} \leq 75$ μg/m^3), lightly polluted (LP, $75 < PM_{2.5} \leq 115$ μg/m^3), moderately polluted (MP, $115 < PM_{2.5} \leq 150$ μg/m^3), heavily polluted (HP, $150 < PM_{2.5} \leq 250$ μg/m^3) and severely polluted (SP, $PM_{2.5} > 250$ μg/m^3), respectively. As expected, the OC and EC concentrations increased with the deterioration of the air quality in the four sites. This result was consistent with a previous study, which indicated that OC and EC became more important when $PM_{2.5}$ concentrations increase in Beijing (Sun et al., 2019). For Shijiazhuang the OC and EC concentrations roughly doubled from heavily polluted days to severely polluted days; this is closely related to the unfavorable meteorological conditions and large emissions at this site. It can further be seen in Fig. 2 that there is some difference in the OC/EC ratios with

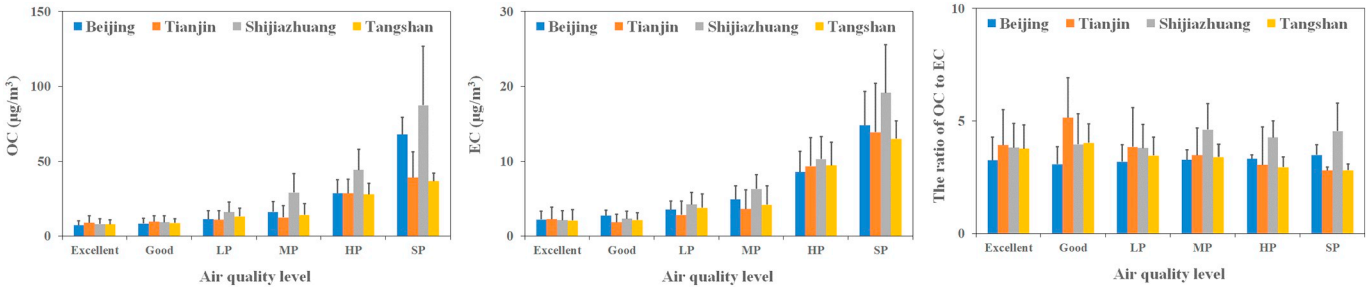

Fig. 2. Variation in OC and EC concentrations and of the OC/EC ratio for different air quality levels.

the variation in air quality levels. The ratios slightly increased with the degradation of air quality in Beijing and Shijiazhuang, while there was some decline with the degradation of air quality in Tianjin and Tangshan. A plausible explanation for the decline in the OC/EC ratio with degrading air quality in Tianjin and Tangshan is that the higher scavenging efficiency for OC than that for EC may lead to lower levels of OC relative to EC during the higher RH condition (Collett Jr et al., 2008), which normally accompanies the pollution episodes (Ji et al., 2014); higher RH conditions frequently occur in Tianjin (days with RH > 80% occurred for 35% of the study period) and Tangshan (days with RH > 80% occurred for 42%), as both cities are adjacent to the sea. On the contrary, due to the drier weather condition in Beijing (days with RH > 80% occurred for 22% of the study period) and Shijiazhuang (days with RH > 80% occurred for 27%), the scavenging of OC in these two cities might be relatively weaker than in Tianjin and Tangshan. In addition, decentralized coal combustion for domestic heating and secondary conversion would still occur although radical control measures were taken to temporarily halt or suspend industrial activities during the severe pollution episodes. Even the secondary formation of OC exacerbated during the severely polluted days as reported by Huang et al. (2014). With the aggravation of the air pollution, both decentralized coal combustion for residential heating and secondary formation played relatively more important roles than vehicular emissions and the scavenging effect, which could result in an increase in the OC/EC ratio (Ji et al., 2018).

3.2. Spatiotemporal variation

3.2.1. Monthly variation

Fig. S2 shows the monthly variation for OC and EC in Beijing, Tianjin, Shijiazhuang, and Tangshan. For OC, the variation is similar at the four sites with the highest concentrations in December and the lowest ones in July or August. The monthly average concentrations in December 2016 were 24.2, 21.4, 75 and 21.1 μg/m^3 for Beijing, Tianjin, Shijiazhuang and Tangshan, respectively, which is explained by the combined effect of large emissions from residential heating, unfavorable meteorological conditions, and more secondary conversion. The lowest monthly average concentrations were 5.2, 5.1, 7.0 and 7.0 μg/m^3 for Beijing, Tianjin, Shijiazhuang and Tangshan, respectively. The largest interquartile range was observed in Shijiazhuang, i.e., 55 μg/m^3 in December 2016, while the lowest one was seen in Shijiazhuang, i.e., 3.4 μg/m^3 in July 2017. Note that the monthly average concentration was slightly larger in June than in the other summer months; this could be attributed to the stronger emission from biomass burning associated with the higher number of fire spots in Beijing, Tianjin and Hebei province as can be seen in Table S5. As reported by Andersson et al. (2015), biomass burning could give rise to OC emission and formation in eastern China.

For EC, the variation in the monthly average concentrations was similar to that of OC with the highest concentrations in December and the lowest ones in July or August. The monthly average EC concentrations in December 2016 were 7.3, 6.9, 15.9 and 7.0 μg/m^3 for Beijing, Tianjin, Shijiazhuang and Tangshan, respectively; these peak concentrations can be attributed to the additional consumption of coal for residential heating and relatively more stagnant meteorological condition during the winter season. The lowest monthly average EC concentrations were 2.1, 1.2, 2.2 and 1.6 μg/m^3 for Beijing, Tianjin, Shijiazhuang and Tangshan, respectively. The largest interquartile range for EC was 12.2 μg/m^3 in December 2016 (in Shijiazhuang) while the lowest one was 1.2 μg/m^3 in July 2017 (in Tianjin). The monthly average concentrations for EC were like those for OC higher in June than in the other summer months. This is again associated with the larger number of fire spots in that month (Table S5), possibly resulting in higher emission from biomass burning.

3.2.2. Seasonal variation

Fig. 3 depicts the seasonal variation for OC and EC during the study period, which appears to be similar at the four sites. OC exhibits a strong seasonality with higher concentrations in autumn and winter and lower ones in spring and summer. In winter, the average OC concentrations and associated standard deviations were 19.0 ± 17.3, 19.4 ± 13.5, 52.4 ± 20.4 and 18.7 ± 2.4 μg/m^3 in Beijing, Tianjin, Shijiazhuang and Tangshan, respectively. The clear difference in OC concentrations observed at the four sites was caused by the difference in energy structure and meteorological conditions. More coal consumption in Shijiazhuang (3872.5 × 10^4 ton coal consumed in 2015, http://paper.people.com.cn/mszk/html/2016-12/05/content_1734113.htm) led to much higher concentrations than in the other three cities. In addition, the lower *WS* at this site gave rise to weaker dispersion, which was unfavorable for blowing the air pollutants away to improve the air quality. Furthermore, vehicular emissions were probably more important in Shijiazhuang than in the other three cities (http://www.hebhb.gov.cn/lishilanmu/hbhbzxd/qtxd/201707/t20170705_54023.html). Thus, the above factors led to the high OC concentrations in Shijiazhuang. The average ratios of OC in winter to OC in summer were 2.6, 2.2, 4.7 and 2.2 for Beijing, Tianjin, Shijiazhuang and Tangshan, respectively.

Like was the case for OC, also EC exhibited a strong seasonality with higher concentrations in autumn and winter and lower ones in spring and summer. In winter, the average EC concentrations and associated standard deviations were 5.6 ± 5.5, 5.8 ± 5.2, 11.3 ± 4.7 and 5.9 ± 5.0 μg/m^3 in Beijing, Tianjin, Shijiazhuang and Tangshan, respectively. More coal consumption and stagnant meteorological conditions gave rise to the high EC concentrations in winter. The lower EC concentrations in spring and summer were caused by relatively higher wind speeds and more precipitation in summer. The average ratios of EC in winter to EC in summer were 2.2, 4.2, 4.7 and 3.2 for Beijing, Tianjin, Shijiazhuang and Tangshan, respectively.

3.2.3. Diurnal variation

Fig. 4 shows the diurnal variation in the OC and EC concentrations in spring, summer, autumn, winter and for the full one-year in Beijing, Tianjin, Shijiazhuang, and Tangshan. Pronounced double-peak diurnal patterns occurred for OC in all four seasons in the four cities. One peak occurred between approximately 6:00 and 10:00, which could result from the combination of vehicular emissions in the morning and

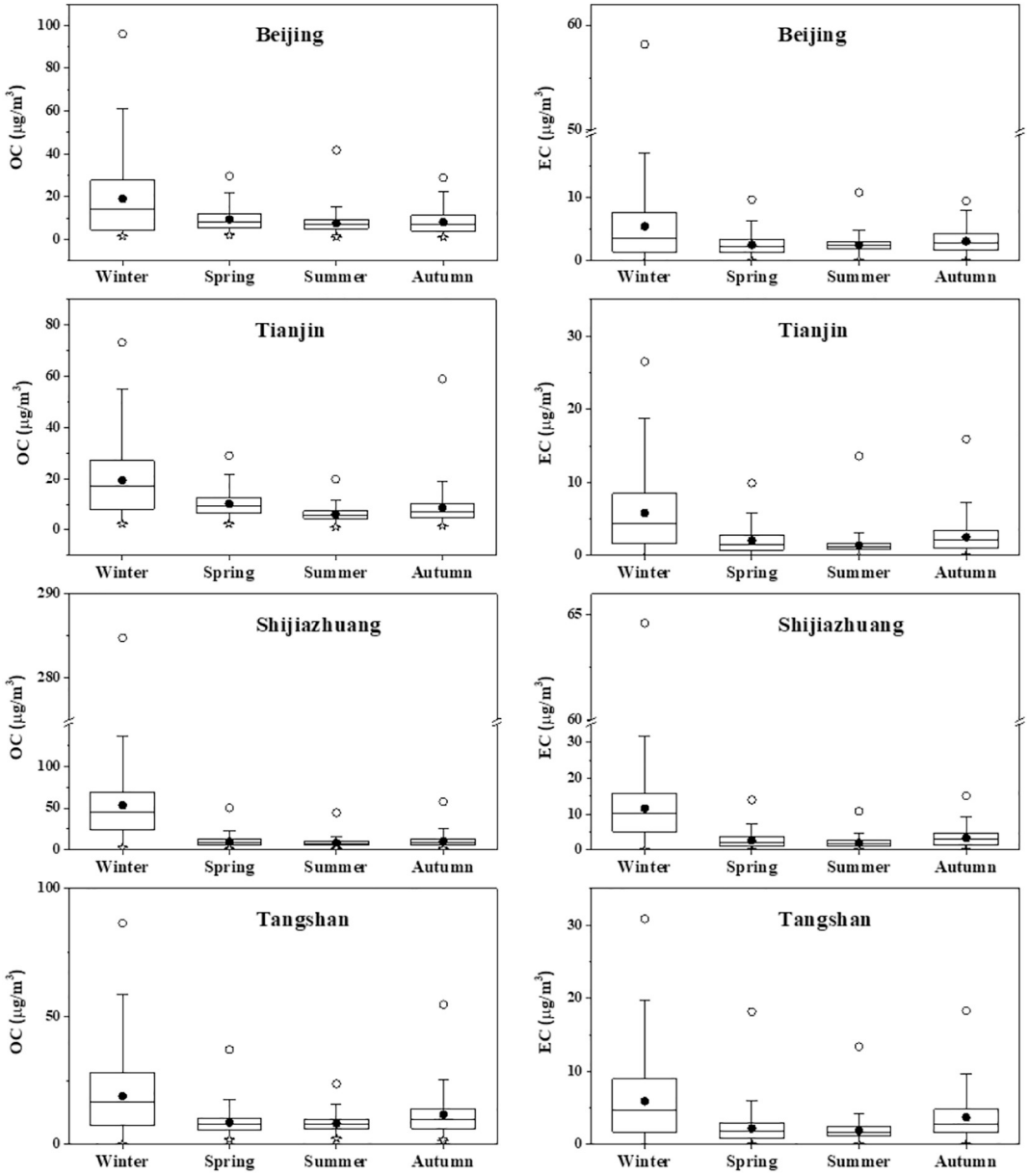

Fig. 3. Box and whisker plots of hourly OC and EC concentrations for the four seasons. The mean (filled circle), median (horizontal line in the box), 25th and 75th percentiles (lower and upper end of the box), 10th and 90th percentiles (lower and upper whiskers), the maximum (hollow circle) and minimum (asterisk) are shown.

secondary OC formation caused by the increasing solar radiation. The other peak occurred during the evening traffic rush hour and even lasted until the next early morning; this peak could be mainly attributed to traffic emissions and the lowering of the planetary boundary layer (PBL). The traffic regulations stipulate that heavy-duty vehicles (HDVs) and heavy-duty diesel trucks (HDDTs) are only permitted to enter the Beijing urban area from 0:00 to 6:00 while HDVs and HDDTs are only permitted to enter the Tianjin, Shijiazhuang and Tangshan urban areas from 20:00 to 6:00. Even stricter measures are taken to ban the HDV and HDDT operation in urban areas when severe haze events occur in autumn and winter; these measures led to the observed EC and OC peaks during the nighttime.

In addition to the influence of the evolution of the PBL (Kleinman et al., 2008), a different emission inventory between day and night may also be responsible for an additional contribution of carbonaceous aerosols during the nighttime. The change in emissions was examined by looking at the diurnal variations of OC/ΔCO and EC/ΔCO ($\Delta CO = C_{CO}$-$C_{CO\ background}$, where C_{CO} is the concentration of CO and $C_{CO\ background}$ is the background concentration of CO, which is calculated as the average of the lowest 10th percentile of the CO mixing ratios observed during the whole study period) (Fig. 5). Although these diurnal variations show obvious spatial variability, a similar pattern is recorded within each city in the four seasons. In Beijing, peaks of OC/ΔCO and EC/ΔCO are observed at 0:00 and 16:00. The additional emission from HDVs and HDDTs in the nighttime enhanced the OC/ΔCO and EC/ΔCO ratios in Beijing. The peaks at 16:00 in summer are attributed to secondary conversion for OC and regional transport of OC and EC (Ji et al., 2016b). The lowest OC and EC concentrations were observed between approximately 10:00 and 16:00 because of incremental solar radiation and the development of turbulent eddies, providing a larger volume for dilution and dispersion of pollutants; hence an OC and EC trough can be observed during this period. For Tianjin, OC/ΔCO and EC/ΔCO showed small day-night variations with a peak occurring almost from 17:00 to 24:00. It suggests that emission from the evening and nighttime traffic was responsible for the increase in OC/ΔCO and EC/ΔCO ratios. In Shijiazhuang and Tangshan, OC/ΔCO and EC/ΔCO showed clear day-night variations. In Shijiazhuang both ratios increased from 9:00, peaked at 20:00, remained high until 24:00

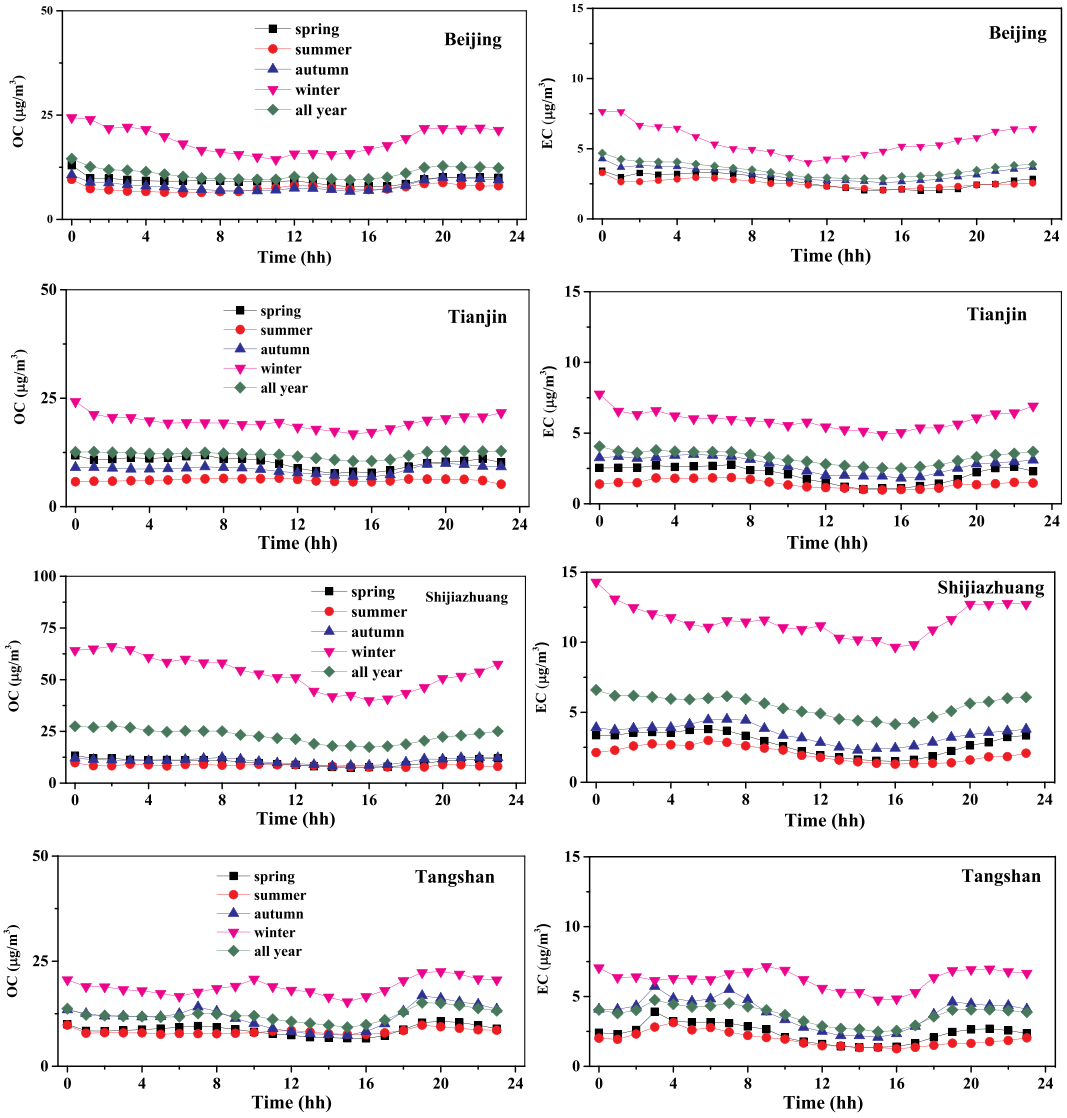

Fig. 4. Diurnal variations in OC and EC in Beijing, Tianjin, Shijiazhuang and Tangshan.

and then decreased. Slightly different from Shijiazhuang, the peaks for OC/ΔCO and EC/ΔCO occurred at 19:00 in Tangshan, possibly indicating that the traffic emission during the evening rush hour contributed more significantly to the enhancement of the OC/ΔCO and EC/ΔCO ratios than was the case during the remainder of the nighttime.

The diurnal variations of the ratios of OC/$PM_{2.5}$ and EC/$PM_{2.5}$ are shown in Fig. 6. These ratios could give detailed information on variations in source strengths for OC and EC since they are not affected by the variation of the PBL height. The diurnal variations of the ratios of OC/$PM_{2.5}$ and EC/$PM_{2.5}$ appear to be similar to, but less pronounced than those of OC and EC. Traffic emission during rush hours is clearly responsible for the peaks in the ratios of OC/$PM_{2.5}$ and EC/$PM_{2.5}$. A study in the Pearl River Delta showed that OC and EC from vehicular emission contribute a lot to $PM_{2.5}$ there (Dai et al., 2015). As shown in Fig. 6, prominent peaks in the ratios of OC/$PM_{2.5}$ and EC/$PM_{2.5}$ were recorded at around 9:00 and 19:00. Additional peaks were also observed in late night, which might be ascribed to emission from HDVs and HDDTs in the nighttime. Note that higher ratios of OC accounting for $PM_{2.5}$ were recorded in the daytime of summer. This was possibly because secondary OC formed in the daytime (Seinfeld and Pandis, 2016). The largest amplitude for the diurnal variation in the OC/$PM_{2.5}$ ratio was recorded in summer for Beijing and Tianjing, in winter for Shijiazhuang and in autumn for Tangshan. That for EC/$PM_{2.5}$ was recorded in summer for Beijing, in spring for Tianjing, in autumn for Shijiazhuang and Tangshan, respectively. The differences could be related to the local emissions in the four cities.

3.3. Comparison of present study with previous measurements in the BTH region

To examine the characteristics and evolution of the air pollution in China, our results were compared to and contrasted with previous measurements covering the past two decades in the BTH region (Table S6). To ensure the comparability of data produced by different analytical methods, a comparison was conducted between measurements conducted by TOT and thermal optical reflectance (TOR) methods with different temperature protocols (Fig. S3, Supplementary material). It was found that the TC results from the offline filter samples (TOR) in the four cities were totally consistent with, but somewhat lower than those from the semi-continuous instruments (TOT). As can be seen in Table S6, our OC and EC concentrations are lower than those recorded in earlier studies. This is consistent with the improvement in air quality achieved by the strict execution of the clean air act setting stringent targets and the policy to restrict coal consumption as of September 2013. It was evident, though, that despite those measures the BTH region of China is still a high emission area of OC and EC. It can be seen

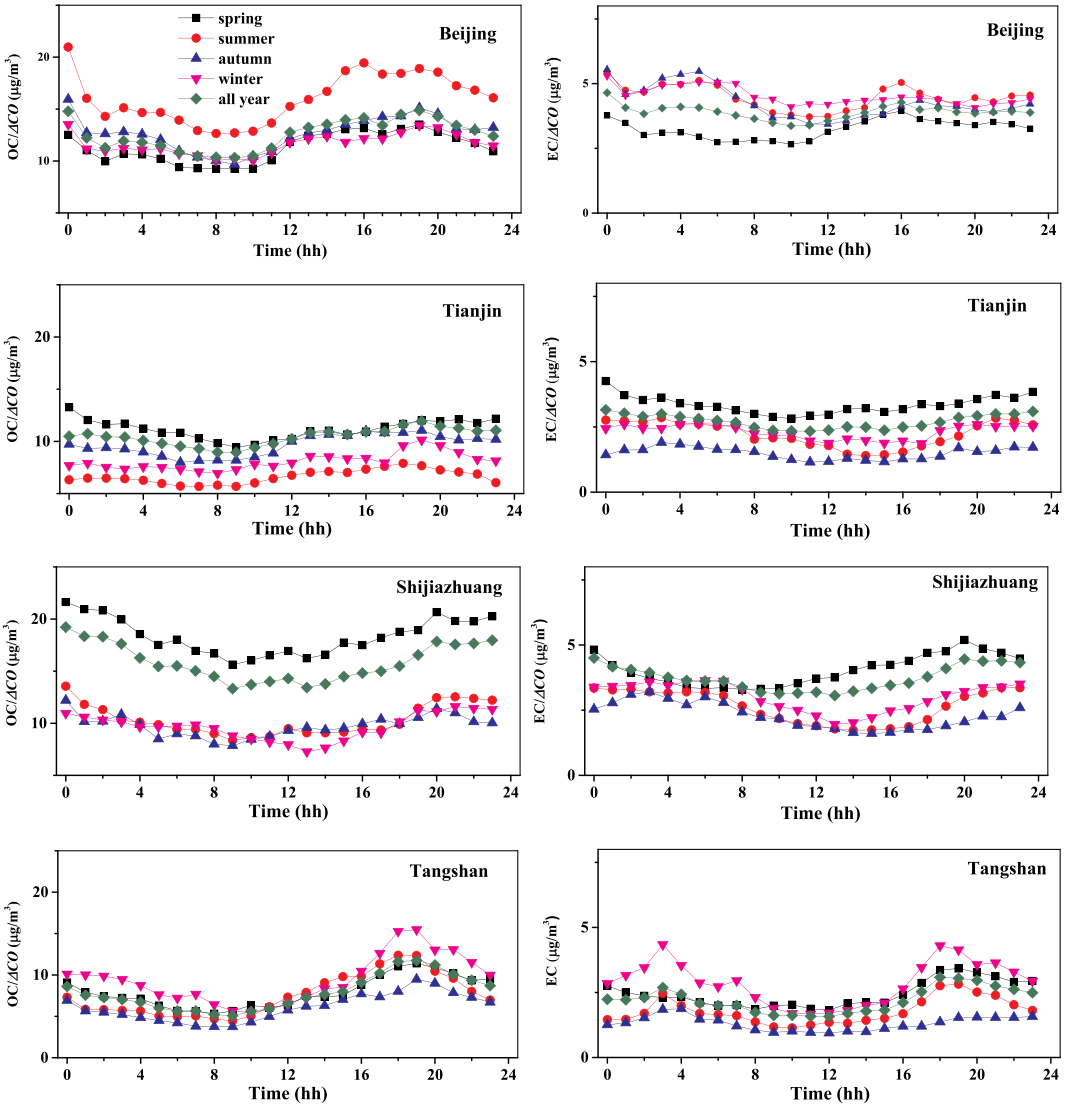

Fig. 5. Diurnal variations in OC/ΔCO and EC/ΔCO in Beijing, Tianjin, Shijiazhuang and Tangshan.

that relatively high concentrations of OC and EC were observed in the BTH region (on average 21.0 and 5.8 μg/m^3 for OC and EC). The ratios of TC to $PM_{2.5}$ were on average 22.9% for the BTH region. Areas with high SO_2 and NO_x emission have lower ratios of TC to $PM_{2.5}$, which is consistent with our earlier finding that secondary inorganic ions accounted for a higher contribution to $PM_{2.5}$ in the areas with more intensive SO_2 and NO_x emission in contrast to TC (Ji et al., 2017).

As for the difference between this study and previous studies, the OC and EC concentrations declined by and large in the BTH region. The OC and EC concentrations roughly declined from 25.3 to 11.0 and from 9.4 to 3.4 μg/m^3, respectively, from 1999 to 2017 in Beijing; they declined from 18.8 to 12.0 μg/m^3 and from 6.9 to 3.1 μg/m^3, respectively, between 2009 and 2017 in Tianjin; they declined from 26.4 to 22.8 μg/m^3 and from 9.7 to 5.4 μg/m^3, respectively, between 2009 and 2017 in Shijiazhuang; and they declined from the range of 19.2–31.8 to 12.1 μg/m^3 and from the range of 6.6–8.8 to 3.5 μg/m^3, respectively, between 2013 and 2017 in Tangshan. Although different measurement methods (IMPROVE-A and NIOSH-like) may cause some uncertainity (10–20%, Chow et al., 2001, Wu et al., 2012) and the sampling periods were also different, it can definitely be concluded that the annual OC and EC concentrations declined in Beijing, Tianjing, Shijiazhuang, and Tangshan. When looking at the seasonal data, note that higher OC and EC concentrations in the BTH region were observed in winter, which was closely associated with intense coal combustion for residential heating and frequent unfavorable meteorology. Consequently, a progressive transition from coal to clean energy is necessary to further improve the air quality in the BTH region. Interestingly, the comparison indicates that the OC and EC concentrations in Shijiazhuang in winter of this study are higher than those in the previous winter, suggesting more precise and effective control measures might need to be taken in a strict manner particularly in winter for this city. In addition, the OC and EC concentrations in winter did not decline in Beijing as would have been expected. Frequent occurrence of unfavorable meteorological conditions, increasing vehicle fleet and enhancement in requirement of residential heating may offset the endeavor of air quality policies (Ji et al., 2014). In the other three seasons, the OC and EC concentrations clearly decreased in Beijing, Tianjin, and Shijiazhuang. The limited research on OC and EC performed in Tangshan made it impossible to draw conclusions on changes in seasonality for that city.

Note that most of the previous studies were based on filter sampling and laboratory analysis and the time resolution was once a day or a week in designed months or specific periods. As a result, possible changes in diurnal variation over the years could not be examined.

3.4. Relationship between OC and EC

The ratio of OC to EC in the aerosol particles is an important parameter, reflecting the source type and transformation characteristics

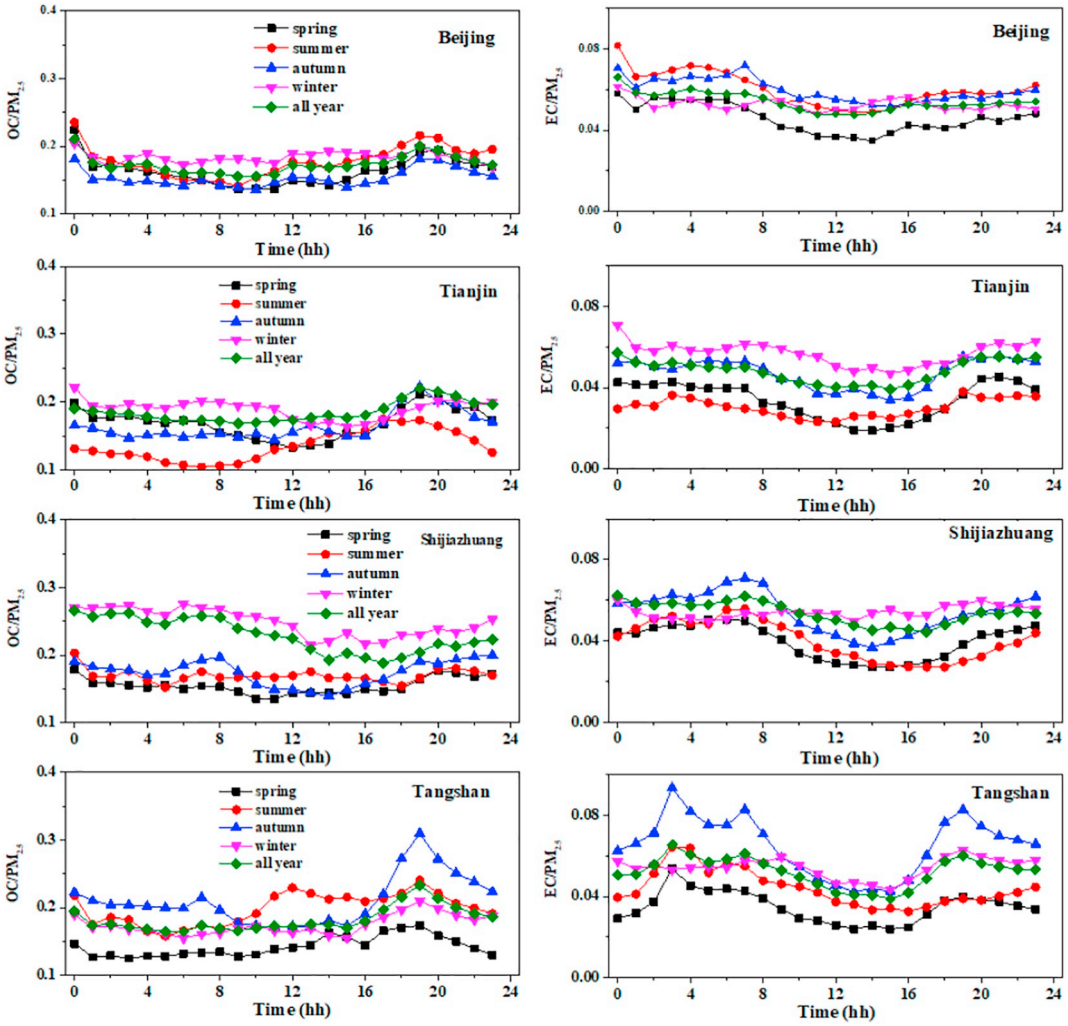

Fig. 6. Diurnal variations in $OC/PM_{2.5}$ and $EC/PM_{2.5}$ in Beijing, Tianjin, Shijiazhuang and Tangshan.

(Blando and Turpin, 2000; Cao et al., 2004). Considering that EC originates mainly from the incomplete combustion of fossil fuels while OC is derived from primary and secondary sources, the slopes and the correlation coefficients of the regression line between OC and EC provide clues on the origin of the carbonaceous aerosol. As shown in Fig. S4, the regression lines of OC versus EC in the four seasons and the full year exhibited significant correlations ($p < 0.001$) for the four sites. The slopes of the regression lines of OC versus EC over the entire year were 3.1, 2.5, 4.1 and 2.4 for Beijing, Tianjin, Shijiazhuang and Tangshan, respectively. There are clear seasonal variations for the slopes, with high values in winter and low values in summer. The slopes were in the range of 2.1–3.1, 1.7–2.6, 2.2–3.8 and 1.6–2.5 in the four seasons for Beijing, Tianjin, Shijiazhuang and Tangshan, respectively. The correlation coefficients also showed seasonal variations with high values in winter and low ones in summer. The correlation coefficients ranged from 0.39 to 0.96, from 0.44 to 0.93, from 0.51 to 0.79 and from 0.30 to 0.89 in the four seasons for Beijing, Tianjin, Shijiazhuang and Tangshan, respectively. Our higher slopes of the regression lines of OC versus EC in wintertime are consistent with those observed in Beijing (Ji et al., 2016a), the Pearl River Delta Region (Duan et al., 2007) and Shanghai (Feng et al., 2009). The relatively strong correlation and high slope may be ascribed to the combined effects of coal combustion and biomass burning for domestic heating and vehicular emission because coal combustion and biomass burning are associated with high OC/EC ratios (Watson et al., 2001; Cao et al., 2007; Huang et al., 2018). For comparison, the following OC/EC ratios have been reported in the literature: 4.0 for fossil fuel combustion, 1.1–5.0 for vehicular emission, 8.5–12 for residential coal combustion and 4.3–80 for biomass burning, respectively (Watson et al., 2001; Cao et al., 2007; Huang et al., 2018). Note that the highest winter slope is observed for Shijiazhuang where coal is dominating in the energy consumption. In summer, a weak correlation is found between OC and EC in all four cities, implying that the dominant OC fraction originated from other sources than those for EC, including long-range transport or local secondary OC formation. In addition, high temperatures favorable for partitioning from the particle phase to the gas phase and a higher efficiency for OC scavenging than for EC during the high RH period gave rise to low slopes in summer.

3.5. Estimation of secondary organic carbon

Quantification of the relative contributions of primary OC (POC) and SOC in atmospheric aerosols is not straightforward. In this study, an innovative MRS method was used to estimate $(OC/EC)_{pri}$ (Wu and Yu, 2016). In this method $(OC/EC)_{pri}$ is obtained through calculating a hypothetical set of $(OC/EC)_{pri}$ and SOC values followed by seeking the minimum of the coefficient of determination (R^2) between SOC and EC. The hypothetical $(OC/EC)_{pri}$ that generates the minimum R^2(SOC, EC) (Fig. 7) then represents the actual $(OC/EC)_{pri}$ ratio if variations of EC and SOC are independent and $(OC/EC)_{pri}$ is relatively constant in the study period. This MRS method has a clear quantitative criterion for the $(OC/EC)_{pri}$ calculation, which avoids the arbitrariness in the selection of data for estimating $(OC/EC)_{pri}$.

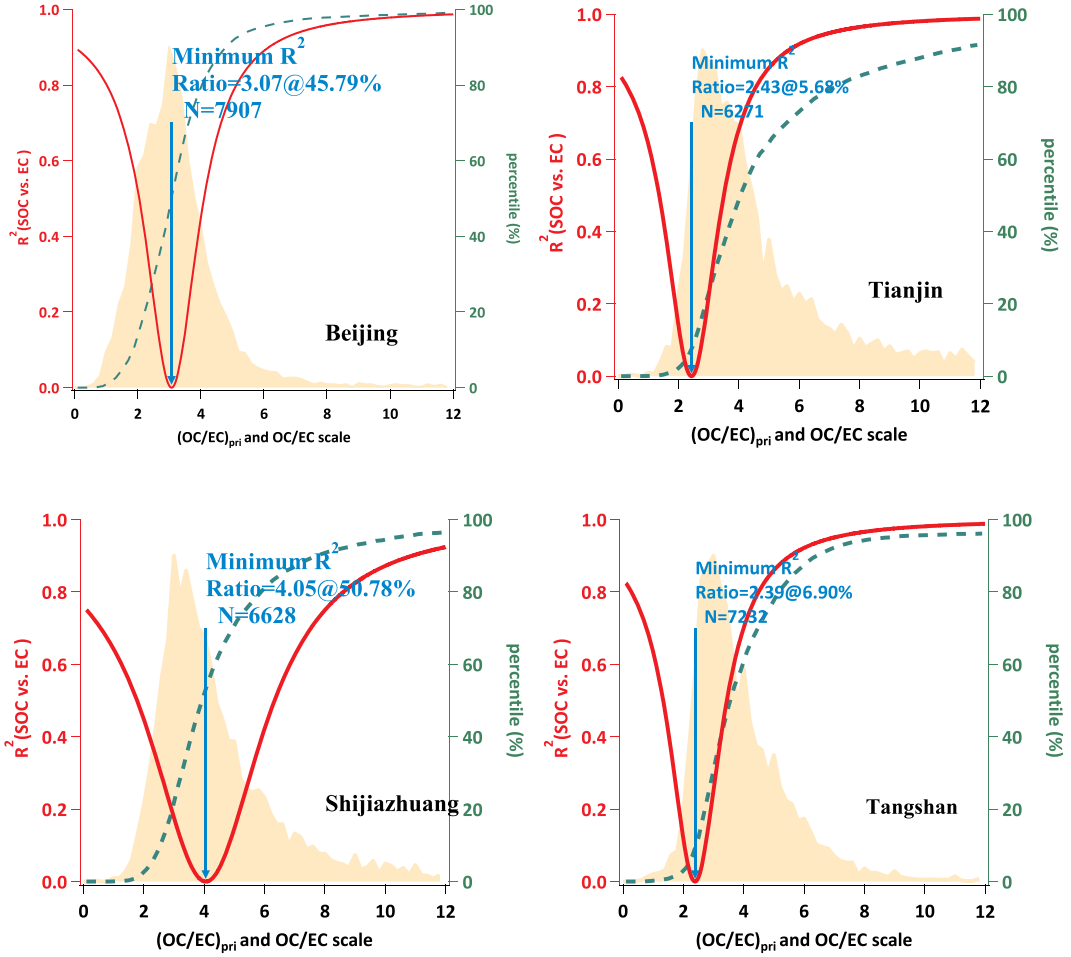

Fig. 7. Illustration of the MRS method to determine $(OC/EC)_{pri}$ using 1 year of hourly OC and EC measurements in Beijing, Tianjin, Shijiazhuang and Tangshan.

For each month at the four sites in this study, $(OC/EC)_{pri}$ values were calculated by the MRS method (Table S7). The SOC concentrations (monthly averages) based on MRS are shown in Table S8. The variation of monthly SOC concentrations was consistent with previous results (Hu et al., 2017). The monthly average MRS SOC data are in the range of 1.8–4.5, 2.5–7.0, 2.9–28.3 and 2.3–6.6 μg/m^3, accounting for 14.7–47%, 21–74%, 21–55% and 17–74% of the OC for Beijing, Tianjin, Shijiazhuang and Tangshan, respectively. As shown in Fig. 8, the highest SOC/OC ratios from MRS were found in the spring (with elevated *T* and low RH) and summer (with elevated *T* and high RH); the higher temperatures in both seasons and the higher RH in summer likely contributed to increased SOC formation via gas-to-particle conversion or heterogeneous reactions and thus larger SOC/OC ratios.

Compared to the MRS SOC/OC ratios for Beijing and Shijiazhuang, high ones are observed for the coastal cities Tianjin and Tangshan (Fig. 8 and Table S9); they were closely associated with lower $(OC/EC)_{pri}$ ratios in the latter two cities. Southerly wind prevailed in Tianjin and Tangshan in summer, which brought humid marine air masses to Tianjin and Tangshan. As indicated in Section 3.2, the higher scavenging efficiency for OC than for EC may lead to lower OC/EC ratios during the higher RH condition (Collett Jr et al., 2008). The meteorological conditions could therefore contribute to lower $(OC/EC)_{pri}$ values. Besides, Tianjin and Tangshan are also important ports and a lot of diesel vehicles are used for transportation of cargo, which result in low OC/EC values (Khan et al., 2012). This also led to lower $(OC/EC)_{pri}$ values. Consequently, the lower $(OC/EC)_{pri}$ values resulted in high SOC concentrations and further led to higher SOC/OC values. The differences in SOC concentrations among the four cities are likely also related to a number of other factors, including differences in types and concentrations of volatile organic compounds (VOCs) and in atmospheric oxidation capacities. For example, in winter the total concentration of VOCs, including aromatics is highest in Shijiazhuang with 1.77×10^3 μg/m^3 (Chang et al., 2015), whereas in summer the total concentration of VOCs, including other VOCs, is highest in Tianjin with 64 ppb (Zhai et al., 2013).

The percentage SOC/OC ratios obtained from MRS in this study are compared with those reported earlier for the BTH region, as found in publications of the past 10 years. The average ratios of SOC/OC based on the MRS method in this study were slightly different from those published in previous studies. For Beijing, our annual percentage SOC/OC ratio of 29% is slightly lower than the overall average of the earlier studies (32%), but our annual percentages for Tianjin (47%) and Shijiazhuang (38%) are substantially larger than the overall averages of the earlier studies, which are 38% for Tianjin and 26% for Shijiazhuang. The above differences can be explained by variations in emission sources over time and differences in methods employed to estimate $(OC/EC)_{pri}$, i.e., MRS versus, e.g., linear regression methods.

As for the seasonal variation in the SOC/OC ratios, it can be seen in Table S9 that we recorded higher ratios in spring and summer than in autumn and winter. This result is in contrast with most of the previous results where lower SOC/OC ratios were recorded in spring and summer than in autumn and winter. As documented by Seinfeld and Pandis (2016), photochemical reactions are more active in spring and summer than in autumn and winter, which is favorable for SOC formation via gas-particle conversion in spring and summer. Considering that SOC formed via photochemical reactions is not correlated with EC and that a high *T* is unfavorable for condensing or absorption of semi-volatile organic compounds (SVOCs) into existing particles, it is

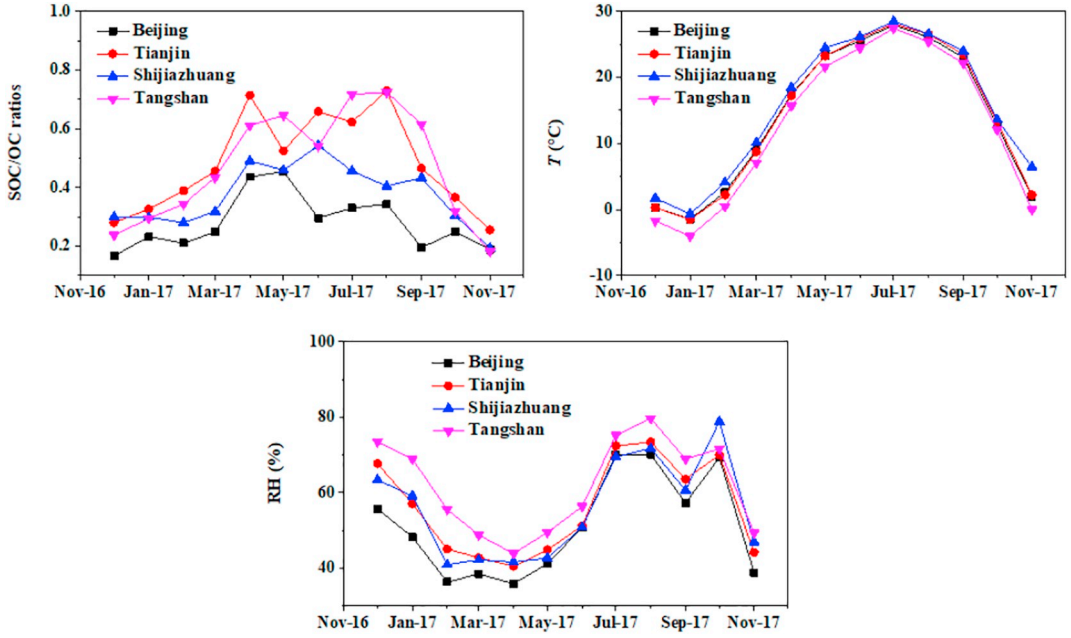

Fig. 8. Monthly average values for the SOC/OC ratio (derived from MRS), T and RH in Beijing, Tianjin, Shijiazhuang and Tangshan.

thought that more reliable results for $(OC/EC)_{pri}$ are obtained with the MRS method for spring and summer. Therefore, our high SOC/OC ratios in those seasons are believed to be more trustworthy than the corresponding ratios in previous studies. On the other hand, a lower *T* is favorable for condensing or absorption of SVOCs into existing particles in autumn and winter. If these SVOCs experience further reactions and thus will become SOC, SOC might be underestimated by the MRS method due to overestimating $(OC/EC)_{pri}$ (Wu and Yu, 2016). This may be the reason for our lower SOC/OC ratios in autumn and winter compared to the corresponding ratios in the previous studies.

3.6. Source area identification

The PSCF results for the hourly resolved OC and EC data provide a visualization of the contribution from regional transport and local emissions in the study areas. The results for the overall data set are shown in Fig. 9, whereas those for the different seasons are given in Fig. S5; the identification of the provinces in these figures is given in Fig. S6. The threshold values used for OC and EC in the PSCF are given in Table S10 for the whole study period and the four seasons. The potential source areas for OC and EC vary among the four study sites and there are also differences in the potential source regions of OC and EC. Furthermore, the source areas vary somewhat with season, as discussed in the Supplementary material.

For Beijing, clear prominent potential source areas of OC and EC are observed, which are mainly located in the central and western areas of Inner Mongolia and even extend to the Mongolian regions. This result is different from previous studies which indicated that emissions from parts of the Hebei, Shandong and Henan provinces played a more important role for the OC and EC concentrations in Beijing (Ji et al., 2018; Hoesly et al., 2018). As mentioned earlier, the Clean Air Act started to be imposed in September 2013. To attain the goals of air quality improvement in the end of 2017 (on average 25% decline in contrast to the annual mean concentrations of 2012), a series of radical control measures, including strict pollution monitoring, industrial production restrictions and tough penalties on polluting enterprises and punishing government officials for failing to mitigate air pollution were executed in the "2 + 26 cities" in Northern China, which includes most cities in the Hebei, Shandong and Henan provinces while Inner Mongolia is not covered. Such a change of the dominant potential source areas might indicate that the effectiveness of the clean air act not only gave rise to an improvement in air quality in this region but also led to some spatial difference in the potential source regions of OC and EC. Besides, there are many industrial activities and a high population density in the central and western areas of Inner Mongolia (http://www.nmgtj.gov.cn/acmrdatashownmgpub/files_nmg_pub/html/nmgtjnj/2015/indexee.htm), which have resulted in high emissions of air pollutants. In detail, coal-fired power plants in northern China are mainly distributed in the Inner Mongolia, Shanxi and Shaanxi provinces (Liu et al., 2015; http://www.greenpeace.org/eastasia/publications/reports/climate-energy/climate-energy-2015/; http://www.epglobe.com/map). An increase in electrical consumption (http://www.stats.gov.cn/english/Statisticaldata/AnnualData/) has been recorded in the BTH region of China. The electricity in the BTH partly originated from coal-fired power plants located in the Inner Mongolia, Shanxi and Shaanxi provinces due to the West-to-East Electricity Transmission Project (Zeng et al., 2016) and this could have led to higher emissions of OC and EC in the Inner Mongolia, Shanxi and Shaanxi provinces. In addition, as shown in Fig. S7, the map of fire spots for the whole study period also showed intense fire spots in the central and western areas of Inner Mongolia. Nonetheless, the gridded emission data (Fig. S1), which show that only a small hotspot of emission of OC and EC is present in the Inner Mongolia, Shanxi and Shaanxi provinces, does not fully agree with the potential contribution areas of OC and EC in Beijing identified in this study. Consequently, in this study, it appears that Inner Mongolia started to overtake the Hebei, Shandong and Henan provinces as the most dominant potential source area for carbonaceous aerosols in Beijing. On the other hand, the contribution from the Hebei, Shandong and Henan provinces is less distinct compared to that from Inner Mongolia and Mongolia, but their contribution to the OC and EC in Beijing is still not negligible, which might be ascribed to the fact that coal and biomass are still widely used for residential cooking and winter heating in this region; besides, the emissions of BC and OC from these other provinces are important based on the gridded emission data in Fig. S1.

For Tianjin, the important potential source areas of OC and EC are mainly located in parts of Inner Mongolia and the north plain of China. Of all the source areas, the southern areas of the Hebei province, small parts of the Shandong province or the adjacent areas of the Shandong and Anhui provinces are the most significant, which is agreement with the gridded emissions of BC and OC in Fig. S1. As reported in the news in China, plenty of small steel factories provide high emissions of air pollutants including of

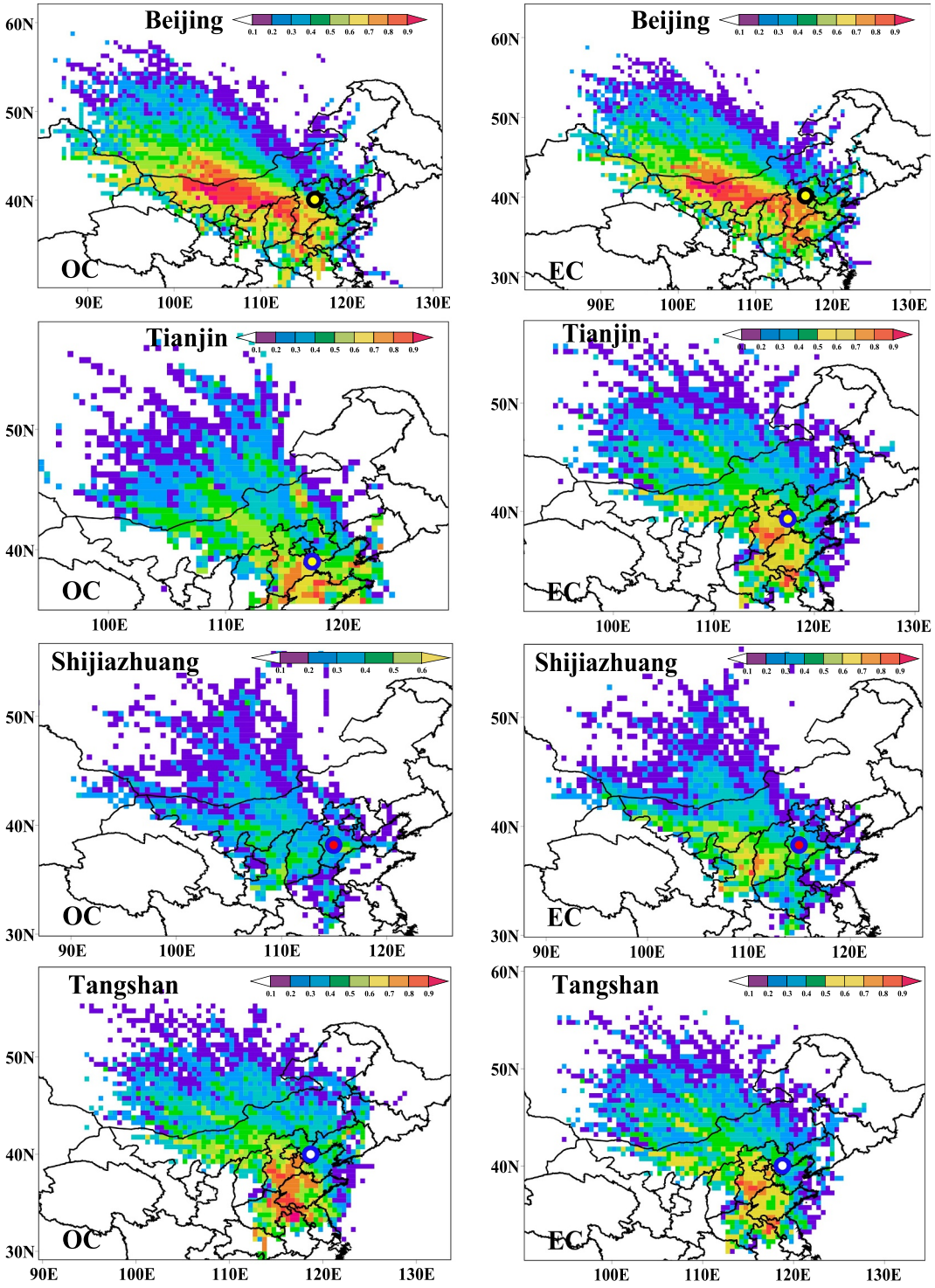

Fig. 9. Potential source areas for OC and EC in the four cities during the study period. The color code denotes the PSCF probability. The location of the sites is indicated with a ○. The identification of the provinces is given in Fig. S6.

OC and EC (http://www.china.org.cn/business/2017-08/31/content_41506899.htm; http://www.sohu.com/a/130963969_465460) in the adjacent areas of the Shandong and Anhui provinces. The rapid economic development, high industrial production accompanied with increased energy consumption, and rise of vehicle fleet numbers resulted in high pollutant emissions from the above-mentioned areas (http://data.stats.gov.cn/english/publish.htm?sort=1). Besides the regional transport, local emissions also contributed substantially to the OC and EC in Tianjin.

For Shijiazhuang, the potential source areas for the full data set are located in the city itself for OC and in the city and the border region of the Shaanxi and Shanxi provinces for EC. The high emission of air pollutants in Hancheng, which is located in that border region, has attracted worldwide attention (https://edition.cnn.com/2018/04/17/health/world-dangerous-air-report-intl/index.html); the pillar industry of domestic economy in that city consists of coal-fired power, coking, sintering and smelting plants. Note that the intensive emissions are mainly contributed by coal combustion (3872.5×10^4 ton in 2015, http://paper.people.com.cn/mszk/html/2016-12/05/content_1734113.htm) and that the vehicular emissions were probably larger in Shijiazhuang than in the other three cities (http://www.hebhb.gov.cn/

lishilanmu/hbhbzxd/qtxd/201707/t20170705_54023.html). The PSCF source locations for both OC and EC for the whole year data set is fully consistent with the BC and OC emission data shown in Fig. S1.

For Tangshan, the prominent potential source areas of both OC and EC are located in Tianjin, southern areas of the Hebei province, and the adjacent areas of the Henan, Shandong and Hebei provinces. However, the prominent potential source areas of EC were less intense than those of OC. Considering that EC and primary OC usually originate from the same sources, the fact that the potential source areas of OC are more intense than those of EC could be caused by the contribution of secondary OC, which originated from the conversion of VOCs from Tianjin, southern areas of the Hebei province, and the adjacent areas of the Henan, Shandong and Hebei provinces during the atmospheric transport. High emissions of VOCs from the above-mentioned areas were recently reported (Li et al., 2016).

4. Conclusions

To obtain a thorough knowledge of OC and EC in the BTH region of China after the strictest emission control measures were implemented, OC and EC in $PM_{2.5}$ were measured on an hourly basis for a full year in Beijing, Tianjin, Shijiazhuang and Tangshan in northern China and an in-depth analysis was performed. The following conclusions can be drawn:

(1) Obvious spatial differences in OC and EC concentrations were found due to differences in energy structure and meteorology. The OC and EC concentrations in the BTH region were still high although a series of air quality control policies have been implemented. Overall, annual average concentrations (± associated standard deviations) of OC and EC (11.0 ± 10.7 and 3.4 ± 3.3, 12.0 ± 9.8 and 3.1 ± 3.6, 22.8 ± 30.6 and 5.4 ± 6.5, and 12.1 ± 9.6 and 3.5 ± 3.6 μg/m^3 for Beijing, Tianjin, Shijiazhuang and Tangshan, respectively) declined in the BTH region but high concentrations of both carbon fractions were still observed in winter (19.0 ± 17.3 and 5.6 ± 5.5, 19.4 ± 13.5 and 5.8 ± 5.2, 52.4 ± 20.4 and 11.3 ± 4.7 and 18.7 ± 2.4 and 5.9 ± 5.0 μg/m^3 for Beijing, Tianjin, Shijiazhuang and Tangshan, respectively).

(2) Clear monthly, seasonal and diurnal variations were found. In brief, a strong seasonality was noted with higher OC and EC concentrations in autumn (8.1 ± 5.1 and 3.1 ± 1.8, 8.6 ± 6.2 and 2.5 ± 2.1, 10.7 ± 7.5 and 3.3 ± 2.4 and 11.8 ± 8.4 and 3.7 ± 3.2 μg/m^3 for Beijing, Tianjin, Shijiazhuang and Tangshan, respectively) and winter, and lower ones in spring (9.3 ± 4.8 and 2.5 ± 1.7, 10.2 ± 4.8 and 2.1 ± 1.8, 10.2 ± 6.1 and 2.7 ± 2.1 and 8.6 ± 4.3 and 2.2 ± 1.9 μg/m^3 for Beijing, Tianjin, Shijiazhuang and Tangshan, respectively) and summer (7.5 ± 3.6 and 2.5 ± 1.0, 8.8 ± 4.5 and 1.4 ± 1.0, 8.5 ± 3.9 and 2.0 ± 1.3 and 8.3 ± 3.0 and 1.9 ± 1.2 μg/m^3 for Beijing, Tianjin, Shijiazhuang and Tangshan, respectively). There was a clear double-peak diurnal pattern in the OC and EC levels, which indicates that there was a substantial impact from traffic on the carbonaceous aerosol levels.

(3) Our concentrations are lower than those reported in earlier studies in the BTH region, which could be ascribed to the execution of the clean air act setting stringent targets and the policy to restrict coal consumption as of September 2013.

(4) A marked spatial difference in SOC/OC ratios was recorded. Our annual percentage SOC/OC ratios were 29%, 47%, 38% and 48% for Beijing, Tianjin, Shijiazhuang and Tangshan, respectively. Note that there was a tendency for our MRS ratios to be larger than previous SOC/OC ratios obtained for the BTH region in the past decade; this is mainly attributable to the difference in estimating SOC as $(OC/EC)_{pri}$ was either estimated by linear regression or set to 2.0 in the earlier studies. Based on the principles applied in the MRS method, it deems to produce more reliable SOC estimates than the regression methods.

(5) Prominent potential source areas of OC and EC were evident for Beijing; they were mainly located in the central and western areas of Inner Mongolia and even extended to the Mongolian regions. Note that adjacent areas of the main provinces in northern China were also prominent potential source areas in the BTH region. The potential source areas of OC and EC agree overall with the spatial distribution of OC and BC in the emission inventory dataset (Fig. S1) and spatial distribution of coal-fired power plants and fire spots.

This multiple-site hourly time-resolved observation of OC and EC evidenced that further control measures for emission reduction in both the particulate and gas phase from coal combustion are needed to mitigate the pollution and the environmental impacts of OC and EC in the region, in particular in winter. Concurrent measurements of OC and EC, VOCs and the chemical composition of OC are required in the future to obtain a comprehensive understanding of the carbonaceous aerosol formation mechanisms under various conditions on the regional scale.

Acknowledgement

This work was supported by the National Key Research and Development Program of China (2017YFC0210000 and 2016YFC0202701), the Beijing Municipal Science and Technology Projects (D17110900150000 and Z171100000617002), the CAS Key Technology Talent Program and the National research program for key issues in air pollution control. The authors would like to thank all members of the LAPC/CERN in IAP, CAS, for maintaining the instruments used in the current study. We also like to thank the USA National Oceanic and Atmospheric Administration (NOAA) for providing the HYSPLIT and TrajStat model.

Appendix A. Supplementary material

Supplementary material to this article can be found online at https://doi.org/10.1016/j.envint.2019.02.034.

References

Andersson, A., Deng, J., Du, K., Zheng, M., Yan, C., Sköld, M., Gustafsson, Ö., 2015. Regionally-varying combustion sources of the January 2013 severe haze events over eastern China. Environ. Sci. Technol. 49 (4), 2038–2043.
Ashbaugh, L.L., Malm, W.C., Sadeh, W.Z., 1985. A residence time probability analysis of sulfur concentrations at Grand Canyon National Park. Atmos. Environ. 19, 1263–1270.
Birch, M.E., Cary, R.A., 1996. Elemental carbon-based method for monitoring occupational exposures to particulate diesel exhaust. Aerosol Sci. Technol. 25, 221–241.
Blando, J., Turpin, B.J., 2000. Secondary organic aerosol formation in cloud and fog droplets: a literature evaluation of plausibility. Atmos. Environ. 34, 1623–1632.
Bond, T.C., Bergstrom, R.W., 2006. Light absorption by carbonaceous particles: An investigative review. Aerosol Sci. Technol. 40, 27–67.
Bond, T.C., Doherty, S.J., Fahey, D.W., Forster, P.M., Berntsen, T., DeAngelo, B.J., Flanner, M.G., Ghan, S., Kärcher, B., Koch, D., Kinne, S., Kondo, Y., Quinn, P.K., Sarofim, M.C., Schultz, M.G., Schulz, M., Venkataraman, C., Zhang, H., Zhang, S., Bellouin, N., Guttikunda, S.K., Hopke, P.K., Jacobson, M.Z., Kaiser, J.W., Klimont, Z., Lohman, U., Schwarz, J.P., Shindell, D., Storelvmo, T., Warren, S.G., Zender, C.S., 2013. Bounding the role of black carbon in the climate system: a scientific assessment. J. Geophys. Res. Atmos. 118 (11), 5380–5552.
Boparai, P., Lee, J., Bond, T.C., 2008. Revisiting thermal-optical analyses of carbonaceous aerosol using a physical model. Aerosol Sci. Technol. 42, 930–948.
Cao, J.J., Lee, S.C., Ho, K.F., Zou, S.C., Fung, K., Li, Y., Watson, J.G., Chow, J.C., 2004. Spatial and seasonal variations of atmospheric organic carbon and elemental carbon in Pearl River Delta region, China. Atmos. Environ. 38 (27), 4447–4456.
Cao, G., Zhang, X., Zheng, F., 2006. Inventory of black carbon and organic carbon emissions from China. Atmos. Environ. 40 (34), 6516–6527.
Cao, J.J., Lee, S.C., Chow, J.C., Watson, J.G., Ho, K.F., Zhang, R.J., Jin, Z.D., Shen, Z.X., Chen, G.C., Kang, Y.M., Zou, S.C., Zhang, L.Z., Qi, S.H., Dai, M.H., Cheng, Y., Hu, K., 2007. Spatial and seasonal distributions of carbonaceous aerosols over China. J. Geophys. Res.-Atmos. 112 (D22), D22S27.
Chang, Q., Luo, Y., Jiang, J.B., Ren, A.L., 2015. Pollution characteristic of VOCs of ambient air in winter and spring in Shijiazhuang City. J. Hebei Univ. Sci. Technol. 36 (3), 330–336.
Chen, F., Zhang, X.H., Zhu, X.S., Zhang, H., Gao, J.X., Hopke, P.K., 2017. Chemical characteristics of $PM_{2.5}$ during a 2016 Winter Haze Episode in Shijiazhuang, China. Aerosol Air Qual. Res. 17 (2), 368–380.
Chow, J.C., Watson, J., Crow, D., Lowenthal, D.H., Merrifield, T., 2001. Comparison of IMPROVE and NIOSH carbon measurements. Aerosol Sci. Technol. 34 (1), 23–34.
Collett Jr., J.L., Herckes, P., Youngster, S., Lee, T., 2008. Processing of atmospheric organic matter by California radiation fogs. Atmos. Res. 87 (3–4), 232–241.
Dai, S., Bi, X., Chan, L.Y., He, J., Wang, B., Wang, X., Peng, P., Sheng, G., Fu, J., 2015.

Chemical and stable carbon isotopic composition of $PM_{2.5}$ from on-road vehicle emissions in the PRD region and implications for vehicle emission control policy. Atmos. Chem. Phys. 15 (6), 3097–3108.
Ding, A.J., Huang, X., Nie, W., Sun, J.N., Kerminen, V.M., Petäjä, T., Su, H., Cheng, Y.F., Yang, X.Q., Wang, M.H., Chi, X.G., Wang, J.P., Virkkula, A., Guo, W.D., Yuan, J., Wang, S.Y., Zhang, R.J., Wu, Y.F., Song, Y., Zhu, T., Zilitinkevich, S., Kulmala, M., Fu, C.B., 2016. Enhanced haze pollution by black carbon in megacities in China. Geophys. Res. Lett. 43 (6), 2873–2879.
Draxler, R.R., Rolph, G.D., 2003. HYSPLIT (HYbrid Single-Particle Lagrangian Integrated Trajectory) Model. NOAA Air Resources Laboratory. Silver Spring, MD (Accessed via NOAA ARL READY Website).
Duan, J.C., Tan, J.H., Cheng, D.X., Bi, X.H., Deng, W.J., Sheng, G.Y., Fu, J.M., Wong, M.H., 2007. Sources and characteristics of carbonaceous aerosol in two largest cities in Pearl River Delta Region, China. Atmos. Environ. 41, 2895–2903.
Feng, Y., Chen, Y., Guo, H., Zhi, G., Xiong, S., Li, J., Sheng, G., Fu, J., 2009. Characteristics of organic and elemental carbon in $PM_{2.5}$ samples in Shanghai, China. Atmos. Res. 92, 434–442.
Giglio, L., 2005. MODIS collection 4 active fire product user's guide: Version 2.2. Available at. http://maps.geog.umd.edu/products/.
Grimmer, G., 2018. Environmental Carcinogens: Polycyclic Aromatic Hydrocarbons. CRC Press.
Gu, J., Bai, Z., Liu, A., Wu, L., Xie, Y., Li, W., Dong, H.Y., Zhang, X., 2010. Characterization of atmospheric organic carbon and element carbon of $PM_{2.5}$ and PM_{10} at Tianjin, China. Aerosol Air Qual. Res. 10, 167–176.
Han, S., Kondo, Y., Oshima, N., Takegawa, N., Miyazaki, Y., Hu, M., Lin, P., Deng, Z., Zhao, Y., Sugimoto, N., Wu, Y., 2009. Temporal variations of elemental carbon in Beijing. J. Geophys. Res. Atmos. 114 (D23), D23202. https://doi.org/10.1029/2009JD012027.
Hansen, J.E., Sato, M., Ruedy, R., Nazarenko, L., Lacis, A., Schmidt, G.A., Russell, G.L., Aleinov, I., Bauer, M., Bauer, S.E., Bell, N., Cairns, B., Canuto, V.M., Chandler, M.A., Cheng, Y., Del Genio, A.D., Faluvegi, G., Fleming, E.L., Friend, A.D., Hall, T.M., Jackman, C.H., Kelley, M., Kiang, N.Y., Koch, D.M., Lean, J., Lerner, J., Lo, K., Menon, S., Miller, R.L., Minnis, P., Novakov, T., Oinas, V., Perlwitz, J., Perlwitz, J., Rind, D., Romanou, A., Shindell, D.T., Stone, P.H., Sun, S., Tausnev, N., Thresher, D., Wielicki, B.A., Wong, T., Yao, M.S., Zhang, S., 2005. Efficacy of climate forcings. J. Geophys. Res. 110 (D18), D18104. https://doi.org/10.1029/2005JD005776.
Hoesly, R.M., Smith, S.J., Feng, L., Klimont, Z., Janssens-Maenhout, G., Pitkanen, T., Seibert, J.J., Vu, L., Andres, R.J., Bolt, R.M., Bond, T.C., Dawidowski, L., Kholod, N., Kurokawa, J., Li, M., Liu, L., Lu, Z.F., Moura, M.C.P., O'Rourke, P.R., Zhang, Q., 2018. Historical (1750–2014) anthropogenic emissions of reactive gases and aerosols from the Community Emissions Data System (CEDS). Geosci. Model Dev. 11 (1), 369–408. https://doi.org/10.5194/gmd-11-369-2018.
Hu, J.L., Wang, P., Ying, Q., Zhang, H.L., Chen, J.J., Ge, X.L., Li, X.H., Jiang, J.K., Wang, S.X., Zhang, J., Zhao, Y., Zhang, Y.Y., 2017. Modeling biogenic and anthropogenic secondary organic aerosol in China. Atmos. Chem. Phys. 17, 77–92. https://doi.org/10.5194/acp-17-77-2017.
Huang, R.J., Zhang, Y., Bozzetti, C., Ho, K.F., Cao, J.J., Han, Y., Han, Y., Daellenbach, K.R., Slowik, J.G., Platt, S.M., Canonaco, F., Zotter, P., Wolf, R., Pieber, S.M., Bruns, E.A., Crippa, M., Ciarelli, G., Piazzalunga, A., Schwikowski, M., Abbaszade, G., Schnelle-Kreis, J., Zimmermann, R., An, Z., Szidat, S., Baltensperger, U., El Haddad, I., Prévôt, A.S., 2014. High secondary aerosol contribution to particulate pollution during haze events in China. Nature 514 (7521), 218–222.
Huang, X.J., Liu, Z.R., Liu, J.Y., Hu, B., Wen, T.X., Tang, G.Q., Zhang, J.K., Wu, F.K., Ji, D.S., Wang, L.L., Wang, Y.S., 2017. Chemical characterization and synergetic source apportionment of $PM_{2.5}$ at multiple sites in the Beijing-Tianjin-Hebei region, China. Atmos. Chem. Phys. 17 (21), 12941–12962.
Huang, Y., Liu, Y., Zhang, L., Peng, C., Yang, F., 2018. Characteristics of carbonaceous aerosol in $PM_{2.5}$ at Wanzhou in the southwest of China. Atmosphere 9 (2), 37.
IARC (International Agency for Research on Cancer), 2010. Some non-heterocyclic polycyclic aromatic hydrocarbons and some related exposures. IARC Monogr. Eval. Carcinog. Risks Hum. 92, 765–771.
IPCC (The Intergovernmental Panel on Climate Change), 2013. Fifth Assessment Report (AR5). http://www.ipcc.ch/report/ar5/wg1/.
Ji, D., Li, L., Wang, Y., Zhang, J., Cheng, M., Sun, Y., Liu, Z.R., Wang, L.L., Tang, G.Q., Hu, B., Chao, N., Wen, T.X., Miao, H.Y., 2014. The heaviest particulate air-pollution episodes occurred in northern China in January, 2013: insights gained from observation. Atmos. Environ. 92, 546–556.
Ji, D.S., Zhang, J.K., He, J., Wang, X.J., Pang, B., Liu, Z.R., Wang, L.L., Wang, Y.S., 2016a. Characteristics of atmospheric organic and elemental carbon aerosols in urban Beijing, China. Atmos. Environ. 125, 293–306.
Ji, D.S., Gao, W.K., Zhang, J., Morino, Y., Zhou, L., Yu, P., Li, Y., Sun, J.R., Ge, B.Z., Tang, G.Q., Sun, Y.L., Wang, Y.S., 2016b. Investigating the evolution of summertime secondary atmospheric pollutants in urban Beijing. Sci. Total Environ. 572, 289–300.
Ji, D.S., Li, L., Pang, B., Xue, P., Wang, L.L., Wu, Y., Zhang, H., Wang, Y., 2017. Characterization of black carbon in an urban-rural fringe area of Beijing. Environ. Pollut. 223, 524–534.
Ji, D.S., Yan, Y.C., Wang, Z.S., He, J., Liu, B., Sun, Y., Gao, M., Li, Y., Cao, W., Cui, Y., Hu, B., Xin, J.Y., Wang, L.L., Liu, Z.R., Tang, G.Q., Wang, Y.S., 2018. Two-year continuous measurements of carbonaceous aerosols in urban Beijing, China: temporal variations, characteristics and source analyses. Chemosphere 200, 191–200.
Jiang, J.B., Chang, Q., Feng, Y., Luo, Y., Li, Z.G., 2017. Seasonal variation of organic carbon and elemental carbon in atmospheric particles in Shijiazhuang. Environ. Monit. Forewarning 9 (2), 41–45.
Junker, C., Liousse, C., 2008. A global emission inventory of carbonaceous aerosol from historic records of fossil fuel and biofuel consumption for the period 1860-1997. Atmos. Chem. Phys. 8 (5), 1195–1207.
Khan, B., Hays, M.D., Geron, C.D., Jetter, J.J., 2012. Differences in the OC/EC ratios that characterize ambient and source aerosols due to thermal-optical analysis. Aerosol Sci. Technol. 46 (2), 127–137.
Kleinman, L.I., Springston, S.R., Daum, P.H., Lee, Y.N., Nunnermacker, L.J., Senum, G.I., Wang, J., Weinstein-Lloyd, J., Alexander, M.L., Hubbe, J., Ortega, J., Canagaratna, M.R., Jayne, J., 2008. The time evolution of aerosol composition over the Mexico City plateau. Atmos. Chem. Phys. 8, 1559–1575.
Li, W., Bai, Z., 2009. Characteristics of organic and elemental carbon in atmospheric fine particles in Tianjin, China. Particuology 7 (6), 432–437.
Li, J., Li, L.Y., Wu, R.R., Li, Y.Q., Bo, Y., Xie, S.D., 2016. Inventory of highly resolved temporal and spatial volatile organic compounds emission in China. Air Pollut. XXIV 207, 79–86.
Li, X., Huang, L., Li, J.Y., Shi, Z., Wang, Y., Zhang, H.L., Ying, Q., Yu, X.N., Liao, H., Hu, J.L., 2019. Source contributions to poor atmospheric visibility in China. Resour. Conserv. Recycl. 143, 167–177.
Liu, F., Zhang, Q., Tong, D., Zheng, B., Li, M., Huo, H., He, K.B., 2015. High-resolution inventory of technologies, activities, and emissions of coal-fired power plants in China from 1990 to 2010. Atmos. Chem. Phys. 15, 13299–13317.
Lupu, A., Maenhaut, W., 2002. Application and comparison of two statistical trajectory techniques for identification of source regions of atmospheric aerosol species. Atmos. Environ. 36, 5607–5618.
Menon, S., Novakov, T., Perlwitz, J., Russell, G., Schmidt, G.A., Tausnev, N., 2005. Earth's energy imbalance: confirmation and implications. Science 308, 1431–1435.
Mills, N.L., Törnqvist, H., Robinson, S.D., Gonzalez, M., Darnley, K., MacNee, W., Boon, N.A., Donaldson, K., Blomberg, A., Sandstrom, T., Newby, D.E., 2005. Diesel exhaust inhalation causes vascular dysfunction and impaired endogenous fibrinolysis. Circulation 112 (25), 3930–3936.
Peng, R.D., Bell, M.L., Geyh, A.S., Mcdermott, A., Zeger, S.L., Samet, J.M., Dominici, F., 2009. Emergency admissions for cardiovascular and respiratory diseases and the chemical composition of fine particle air pollution. Environ. Health Perspect. 117 (6), 957–963.
Poirot, R.L., Wishinski, P.R., 1986. Visibility, sulfate and air mass history associated with the summertime aerosol in northern Vermont. Atmos. Environ. 20, 1457–1469.
Polissar, A.V., Hopke, P.K., Paatero, P., Kaufmann, Y.J., Hall, D.K., Bodhaine, B.A., Dutton, E.G., Harris, J.M., 1999. The aerosol at Barrow, Alaska: long-term trends and source locations. Atmos. Environ. 33, 2441–2458.
Polissar, A.V., Hopke, P.K., Harris, J.M., 2001. Source regions for atmospheric aerosol measured at Barrow, Alaska. Environ. Sci. Technol. 35, 4214–4226.
Seinfeld, J.H., Pandis, S.N., 2016. Atmospheric Chemistry and Physics: From Air Pollution to Climate Change. John Wiley & Sons, Hoboken.
Sun, Y., Wang, Z.F., Du, W., Zhang, Q., Wang, Q., Fu, P., Pan, X., Li, J., Jayne, J.T., Worsnop, D.R., 2015. Long-term real-time measurements of aerosol particle composition in Beijing, China: seasonal variations, meteorological effects, and source analysis. Atmos. Chem. Phys. 15 (17), 10149–10165.
Sun, J.J., Liang, M.J., Shi, Z.H., Shen, F.Z., Li, J.Y., Huang, L., Ge, X.L., Chen, Q., Sun, Y.L., Zhang, Y.L., Chang, Y.H., Ji, D.S., Ying, Q., Zhang, H.L., Kota, S.H., Hu, J.L., 2019. Investigating the $PM_{2.5}$ mass concentration growth processes during 2013–2016 in Beijing and Shanghai. Chemosphere. 221, 452–463.
Turpin, B.J., Huntzicker, J.J., 1995. Identification of secondary organic aerosol episodes and quantitation of primary and secondary organic aerosol concentrations during SCAQS. Atmos. Environ. 29 (23), 3527–3544.
Wang, Y.Q., Zhang, X.Y., Draxler, R.R., 2009. TrajStat: GIS-based software that uses various trajectory statistical analysis methods to identify potential sources from long-term air pollution measurement data. Environ. Model. Softw. 24 (8), 938–939.
Wang, G., Cheng, S., Li, J., Lang, J., Wen, W., Yang, X., Tian, L., 2015a. Source apportionment and seasonal variation of $PM_{2.5}$ carbonaceous aerosol in the Beijing-Tianjin-Hebei Region of China. Environ. Monit. Assess. 187 (3), 143.
Wang, G., Han, L.H., Cheng, S.Y., Lang, J.L., Wen, W., Liu, C., Yang, X.W., 2015b. Characteristics and source apportionment of carbonaceous aerosols during summer period in typical cities. J. Beijing Univ. Technol. 41 (3), 452–460.
Watson, J.G., Chow, J.C., Houck, J.E., 2001. $PM_{2.5}$ chemical source profiles for vehicle exhaust, vegetative burning, geological material, and coal burning in Northwestern Colorado during 1995. Chemosphere 43, 1141–1151.
Wen, W., Cheng, S., Liu, L., Chen, X., Wang, X., Wang, G., Li, S., 2016. $PM_{2.5}$ chemical composition analysis in different functional subdivisions in Tangshan, China. Aerosol Air Qual. Res. 16, 1651–1664.
Wu, C., Yu, J.Z., 2016. Determination of primary combustion source organic carbon-to-elemental carbon (OC/EC) ratio using ambient OC and EC measurements: secondary OC-EC correlation minimization method. Atmos. Chem. Phys. 16 (8), 5453–5465.
Wu, C., Ng, W.M., Huang, J.X., Wu, D., Yu, J.Z., 2012. Determination of elemental and organic carbon in $PM_{2.5}$ in the Pearl River Delta Region: inter-instrument (Sunset vs. DRI Model 2001 thermal/optical carbon analyzer) and inter-protocol comparisons (IMPROVE vs. ACE-Asia protocol). Aerosol Sci. Technol. 46 (6), 610–621.
Zeng, M., Peng, L.L., Fan, Q.N., Zhang, Y.J., 2016. Trans-regional electricity transmission in China: status, issues and strategies. Renew. Sust. Energ. Rev. 66, 572–583.
Zhai, Z.X., Zou, K.H., Li, W.F., Wang, G., Zhai, Y.C., 2013. Pollution characterization of volatile organic compounds in ambient air of Tianjin downtown. Environ. Sci. 34 (12), 4513–4518.
Zhao, P., Dong, F., Yang, Y., 2013. Characteristics of carbonaceous aerosol in the region of Beijing, Tianjin, and Hebei, China. Atmos. Environ. 71, 389–398.